

Fig. 4 Sketch showing processes of vertical transport in the upper ocean boundary layer. *a*, Breaking waves: (i), injecting a downward jet of warmer near-surface water and bubbles, (ii), later development. The near-surface water is carried forward by the momentum transferred from the breaking wave. The warm bubble-filled plume is tilted. (See ref. 3, Figs 5c, 6 and 12b for sonographs of tilted bubble clouds.) The lower interface is gravitationally stable; the upper is unstable. *b*, Langmuir circulation. Bubbles formed by waves breaking between the wind rows are carried into the downwelling zones by the circulation. *c*, Eddies and temperature ramps. The instruments were towed upwind, and the ramps are observed as the sensors pass from cold (bubble deficient) water to warm water.

lag of the temperature maxima with depth seen in Fig. 3a(ii) suggests a pronounced presence of shear (see Fig. 4a(ii)) in conditions of increasing wind and more frequent wave breaking. We cannot unambiguously distinguish between these two processes in the present data set, although the frequency of encounter of bands of bubbles formed by Langmuir circulation is expected to be small since the tows were made upwind and so mainly parallel to the wind rows.

The third process is one associated with eddies with axes predominantly aligned cross-wind (in contrast with the downwind alignment of the Langmuir circulations)¹⁴. These lead to temperature ramps^{15,16}, that is, tilted regions of high temperature gradient. The generation mechanism is unclear, possibly an instability of the vertical shear¹⁷. Figure 3b and c are consistent with the pattern sketched in Fig. 4c, the delay in the temperature increase of 2–4 s between 2.4 and 6.6 m corresponding to a ramp slope of 27 to 46° to the horizontal. This is consistent with previous observations¹⁴. Figure 3b and c shows that the temperature ramps are narrow with large changes occurring in 0.5 s (about 1 m horizontally). They are also structured, following and being followed by, thin 'overshoot' regions of lower or higher temperature which often have corresponding lower or higher sonar scattering.

The presence of temperature ramps leads to a skewness, *S*, of the temperature gradient, dependent on the direction of the tow relative to the wind¹. The observed mean value of *S* decreased from 0.55 at 1.4 m depth to 0.38 at 2.7 m, with an average of 0.44, for towing angles θ within 20° of the wind. The average was less, 0.16, for $25^\circ > \theta > 35^\circ$ and also less, but more variable, at $\theta = 0$ below 2.7 m.

The correlation of bubbles and temperature suggests that the turbulence induced by breaking waves may be related to the formation of temperature ramps, the evolution illustrated in Fig. 4a. The upper boundary of the sheared, and tilted, warm bubble cloud is gravitationally unstable through the contributions to density of both heat and bubbles and thus diffuses more rapidly than the lower boundary, a process leading to skewness in the horizontal temperature gradients. If this is so, the symmetrical signals seen in Fig. 3a(i) may be representative of clouds shortly after their generation (for example, at a time very much less than the reciprocal of the vertical shear) whilst the signals associated with temperature ramps, Fig. 3b, are typical of a later stage of evolution. An experiment is presently planned in which these processes can be examined in more detail using a submarine carrying turbulence probes, temperature sensors and upward-looking as well as side-scan sonar to follow the evolution of bubble clouds from their production by breaking waves.

We thank Alan Packwood for his help in developing the towed spar, and Paul Haines for processing the raw data. The data were collected from MV *Sea Searcher* and the work was supported by the Ministry of Defence Procurement Executive under an agreement with the Admiralty Research Establishment, Portland.

Received 4 February; accepted 16 April 1987.

1. Thorpe, S. A. *Nature* **318**, 519–522 (1985).
2. Hall, A. J. & Packwood, A. R. *IOS Internal Rep.* (1987).
3. Thorpe, S. A. *Phil. Trans. R. Soc. A* **304**, 155–210 (1982).
4. Thorpe, S. A. & Hall, A. J. *Cont. Shelf. Res.* **1**, 353–384 (1983).
5. Thorpe, S. A., Hall, A. J., Packwood, A. R. & Stubbs, A. R. *Cont. Shelf. Res.* **4**, 597–607 (1985).
6. Thorpe, S. A. *J. phys. Oceanogr.* **16**, 1462–1478 (1986).
7. Kolovayev, P. A. *Oceanology* **15**, 659–661 (1976).
8. Johnson, B. D. & Cooke, R. C. *J. geophys. Res.* **84**, 3761–3766 (1979).
9. Farmer, D. M. & Lemmon, D. D. *J. phys. Oceanogr.* **14**, 1762–1778 (1984).
10. Su, M., Green, A. W. & Bergin, M. T. in *Gas transfer at Water Surfaces* (eds Brutsaert, W. & Jirka, G. H.) 211–219 (Reidel, Dordrecht, 1984).
11. Leibovich, S. A. *Rev. Fluid Mech.* **15**, 391–427 (1983).
12. Thorpe, S. A. *J. Fluid Mech.* **15**, 391–427 (1984).
13. Thorpe, S. A. & Hall, A. J. *J. Fluid Mech.* **114**, 237–250 (1982).
14. Thorpe, S. A. & Hall, A. J. *J. Fluid Mech.* **101**, 687–703 (1980).
15. Antonia, R. A., Chambers, A. J., Friehe, C. A. & Van Atta, C. W. *J. Atmos. Sci.* **36**, 99–108 (1979).
16. Gibson, C. H., Friehe, C. A. & McConnell, S. O. *Phys. Fluids Suppl.* **20**, 156–167 (1977).
17. Thorpe, S. A. *J. geophys. Res.* **83**, 2875–2885 (1978).

The surface windfield over the Antarctic ice sheets

Thomas R. Parish* & David H. Bromwich†

* Department of Atmospheric Science, University of Wyoming, Laramie, Wyoming 82071, USA

† Byrd Polar Research Center, The Ohio State University, Columbus, Ohio 43210, USA

The intense radiative cooling of air over the ice slopes of Antarctica generates a surface wind regime that is strongly controlled by topography, and plays a key role in determining the behaviour of the atmosphere and ocean in high southern latitudes^{1–7}. Resultant surface winds are intimately linked to the orientation of the ice terrain (Fig. 1) and display the highest degree of persistence found on Earth. The close coupling between wind and topography allows estimation of the former if the latter is known with some precision. Here we report on time-averaged, near-surface airflow over the Antarctic continent during winter diagnosed from a recent, accurate synthesis of terrain slopes and from estimates of the lower atmospheric temperature structure. The simulated drainage pattern exhibits strong spatial variability with the airflow concentrated into several zones near the coastal margin. These confluence regions are responsible for strong persistent katabatic winds over downstream coastal stretches and are indicative of zones of greatest katabatic potential.

Observational and theoretical studies of gravity-driven slope flows (katabatic winds) are numerous. Ball⁸ points out that the magnitude of terrain-induced pressure gradient is directly proportional to both the steepness of the terrain and the strength of the temperature inversion in the lower atmosphere. Lettau and Schwerdtfeger⁹ refer to this force as the 'sloped-inversion' pressure gradient force to emphasize the interaction between the radiatively forced temperature inversion and the sloping terrain. Other forces which shape the near-surface windfield include the Coriolis force and the frictional force. Large-scale pressure gradients associated with cyclonic storms are probably only of secondary importance because most are situated in the zone of intense thermal contrast between the peripheral ice margins and open ocean and rarely penetrate deep into the Antarctic interior. The strongest winds occur over the steep coastal perimeter where slopes exceed 10^{-2} within the first 150 km inland; they blow almost directly downslope. Winds over the gently sloping continental interior are of more moderate strength and are directed at angles of 40–60° from the fall line. Lettau and Schwerdtfeger⁹ note such interior flows represent a quasi-geostrophic, near-equilibrium wind regime. The term 'inversion' wind has been coined to describe the steady interior surface windfield and to underscore dynamic differences between interior slope flows and the strongly time-dependent coastal 'katabatic' winds.

Although the first-order importance of terrain on the Antarctic surface wind regime has been acknowledged for many years, accurate topographic mapping of the ice contours has only recently been undertaken. Of interest is the series of radio echo soundings carried out by the Scott Polar Research Institute during the past decade. The most refined and up-to-date Antarctic ice topography is presented in Drewry¹⁰, merging the radio echo sounding data with balloon, satellite and oversnow barometric altimetry. The resulting ice contours are thought to be accurate to within approximately ± 30 m, far surpassing the accuracy of previous topographic maps. The importance of refined, precise ice topography maps in understanding the near-surface wind regime over the Antarctic continent cannot be over-emphasized. Parish¹¹ and Parish and Bromwich³ have shown that a realistic diagnosis of the drainage pattern of near-surface winds over the Antarctic continent is possible provided accurate topographic information is available and reasonable estimates of the structure of the temperature inversion are used. The time-averaged streamline maps presented in the above-mentioned works were constructed from the simple steady-state model of Ball⁸ which describes the wind as a balance between the sloped-inversion pressure gradient force, Coriolis force and friction. The steady nature of Antarctic gravity-driven flows over all except the steepest coastal slopes implies a near balance of forces, and the simple Ball model appears to be sufficient for resolving the basic qualitative characteristics of the surface windfield under such conditions. Simulated drainage streamlines over West Antarctica³ and parts of East Antarctica^{11,5} compare favourably with resultant wind directions at interior stations as well as observed sastrugi orientations; sastrugi are streamlined ridges on the snow surface formed by and parallel to the predominant wind.

With the recent completion of a refined topographic map of Antarctica, it is now possible to simulate the time-averaged streamlines of cold air drainage over the entire continent. This is significant because the picture of the surface wind regime will provide *a priori* knowledge of the larger-scale drainage pattern in which a particular site is embedded without the necessity of a costly period of *in situ* measurements. In addition, such a simulation will allow a qualitative estimation of the intensity and persistence of katabatic winds. To diagnose the time-averaged windfield, the entire continent has been digitized to a grid scale of 50 km. This space scale resolves nearly all detail revealed on the Drewry map. Estimates for the temperature inversion over the continent were obtained from the climatologi-

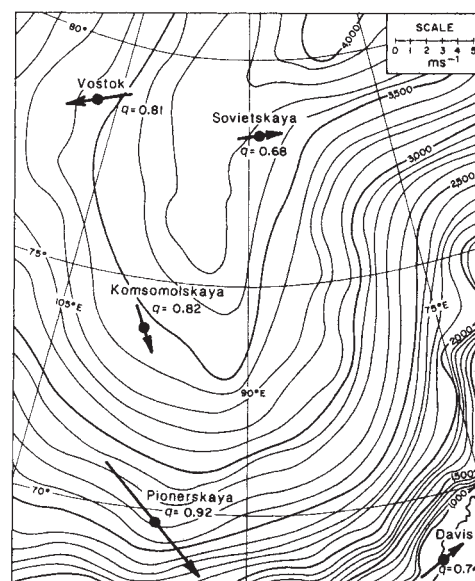


Fig. 1 Annual resultant wind vectors for stations about central ridge in East Antarctica. The symbol q refers to the directional constancy of the wind, the ratio between the vector resultant speed and the mean wind speed. Constancy values near 1 indicate that the airflow is almost exclusively unidirectional.

cal results illustrated in Schwerdtfeger¹². Using the above parameters as the key inputs into the Ball model, equations for the steady motion were solved at each grid point and analyses of the flow directions were then made. To test the sensitivity of the results, a number of runs were carried out, each with a slightly different specification of the inversion strength. The larger-scale drainage features were found to be relatively insensitive to moderate changes in the temperature inversion although the orientation of the drainage patterns do change somewhat in response to the inversion strength differences. This internal consistency was seen in earlier simulations³ and offers testimony to the viability of the simple Ball model in diagnosing qualitative features of Antarctic drainage flows.

Results of the time-averaged near-surface drainage flow pattern from the Ball model are illustrated in Fig. 2. The outstanding feature illustrated in the simulation is the high degree of non-uniformity in the drainage field. The streamlines do not display radially uniform behaviour but rather show a number of clearly defined areas of strong confluence and diffluence. Such patterns have major implications regarding katabatic wind potential and will be discussed in detail later.

Verification of the streamline pattern illustrated in Fig. 2 is understandably difficult owing to the sparse data network over the Antarctic interior. Wind records are available for only about a dozen manned stations in the interior although this data source is currently being supplemented by a number of automatic weather stations (AWS) scattered throughout Antarctica, including several in the continental hinterland. In addition, sastrugi orientation can be used as a proxy indicator of the flow direction. To illustrate the relationship between observed wind direction with the surface streamline simulation in Fig. 2, a composite map has been prepared (Fig. 3) in which resultant wind directions from manned stations and AWS (open arrows) and sastrugi orientations (bold arrows) are plotted relative to a representative number of streamlines from Fig. 2. Previously evaluated sastrugi directions^{3,5,13} have been supplemented by the extensive observations contained within the Japanese Antarctic Research Expedition (JARE) data reports and by data collected during the Australian National Antarctic Research Expeditions (ANARE) traverses. Whenever possible sastrugi directions were

Fig. 2 Time-averaged near-surface wintertime streamlines (heavy lines) of cold air drainage over Antarctica. Thin lines are ice-sheet elevation contours in meters.

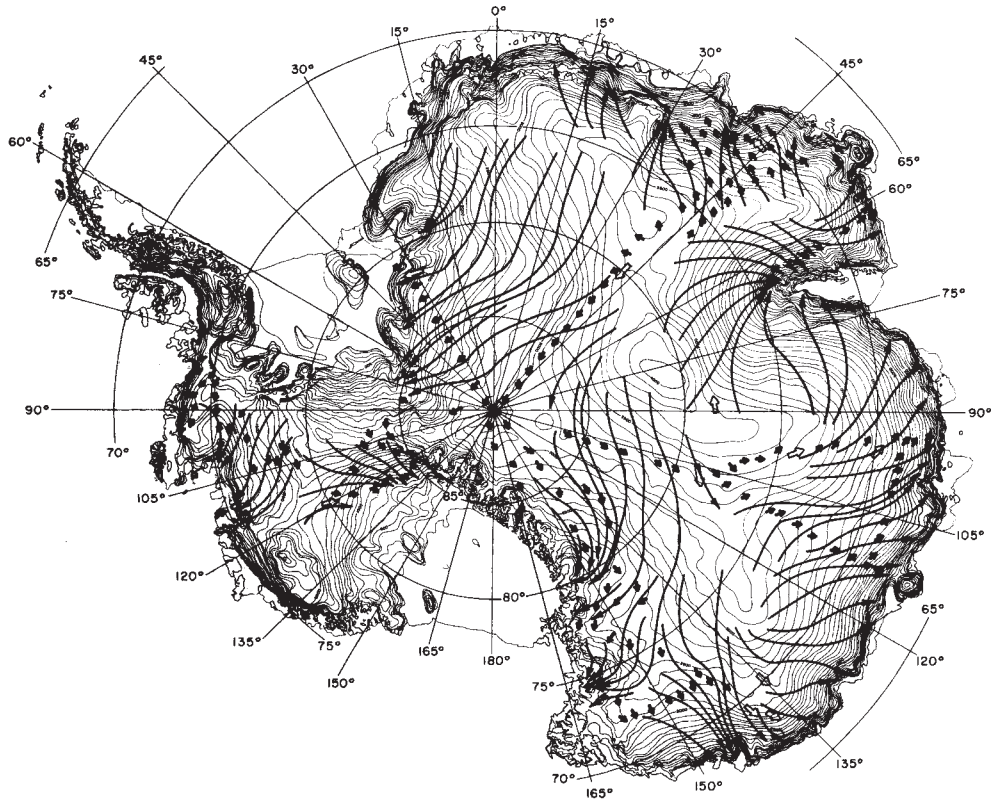
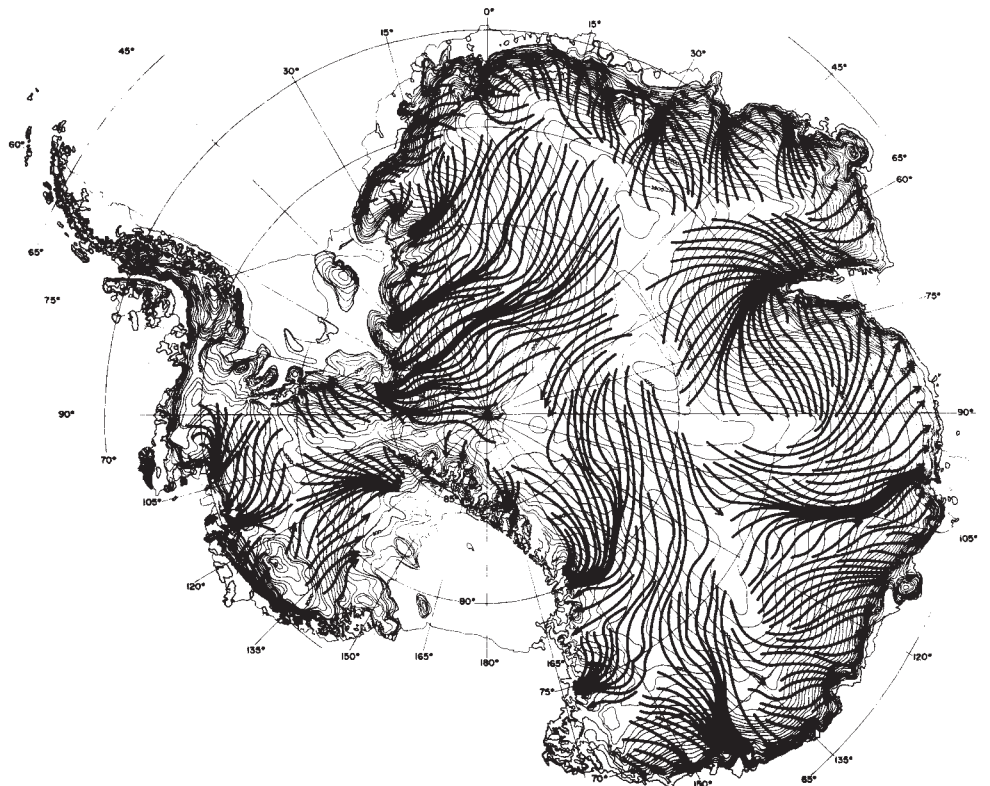


Fig. 3 Composite map of observed annual resultant wind directions (open arrows) and sarrugi orientations (bold arrows) with streamlines of Fig. 2.



averaged in space and time. Orientations clearly attributable to blizzard-induced snow dunes¹³ have been excluded.

In general, it can be concluded from Fig. 3 that the time-averaged surface streamlines are indeed representative of the large-scale surface windfield. In particular, the wind directions obtained from station data are seen to be highly correlated with the inferred drainage pattern. In certain sections (along the 45° E meridian, for example), sastrugi orientations suggest that the simulated streamlines may be directed too sharply down the fall line. Wind and sastrugi observations taken by E. Mosley-Thompson at 84° S, 43° E during December 1986 indicate that many sastrugi directions over the highest parts of the East Antarctic ice sheet, which were mostly collected during the austral summer, reflect the weaker slope flows of the warm period rather than the stronger, more downslope winter winds which have been modelled. It can be concluded with some confidence that the simulated drainage pattern of Fig. 2 is consistent with observations and therefore is probably a good qualitative estimate of the near-surface time-averaged windfield over the Antarctic ice sheets.

The highly irregular drainage pattern is extremely important in understanding the katabatic regime. A serious limitation to the persistence and intensity of katabatic flow is the supply of negatively-buoyant air upslope in the continental interior. Lettau and Schwerdtfeger⁹ note that even moderate katabatic drainage rapidly exhausts cold air reserves 'as, similarly, the bursting of a dam drains a water reservoir'. The strongly time-dependent behaviour of katabatic flow observed along coastal stretches of Antarctica supports the notion of the importance of such a cold air supply. The episodic high-intensity katabatic surges correspond to the cyclical period of discharging of the cold air reservoir upslope and the subsequent recharging of the katabatic potential. The spatial irregularity of the drainage pattern in the interior of the continent acts to modulate the periodicity of the katabatic regime. Numerical simulations have shown that the available cold air supply reservoir can be significantly enhanced along axes of convergence of air currents¹⁴. In turn, the katabatic regime downslope of this streamline confluence zone becomes intensified and more persistent. Observations have clearly revealed the sensitivity of katabatic flow to interior confluence zones.

The most striking connection is seen in Adelie Land, encompassing the stations of Cape Denison (67.0° S, 142.7° E) and Port Martin (66.8° S, 141.4° E). Cape Denison, the "Home of the Blizzard", was the base camp for the Australasian Antarctic Expedition of 1911-14. Observations of the intense katabatic wind taken during the two-year stay were met with scepticism on the group's return to Australia. Subsequent recalibration of the anemometer as well as the French expedition some 40 years later to nearby Port Martin where similar extreme katabatic wind conditions were encountered have given testimony to the original data set. This coastal section of Adelie Land experiences the strongest and most persistent surface winds on the face of the Earth. Observations at Cape Denison show that the average wind speed is about 19.5 m s⁻¹ (37.9 knots). Mather and Miller¹³ suggest the Adelie Land katabatic winds are about 70% stronger than average. As is clearly revealed in Fig. 2, cold air drainage streamlines upslope of Cape Denison and Port Martin display a strongly confluent pattern. It is believed that this confluence channel with the correspondingly large cold air supply is the fundamental cause of the anomalously intense katabatic regime along the Adelie Land coast.

The association between zones of drainage current convergence in the interior and strong katabatic winds near the coast is further supported by the wind record at Terra Nova Bay (74.9° S, 163.7° E), the region where Scott's Northern Party was forced to winter during 1912. Bromwich and Kurtz¹⁵ reanalysed the party's observations; they conclude that the katabatic winds at Terra Nova Bay are anomalously intense and responsible for the formation of a polynya (open water area) which persists

through each winter. In addition, measurements from an AWS located within the Terra Nova Bay region^{16,17} for the autumn months February, March and April 1984 and 1985 show the average wind speed to be about 17 m s⁻¹ (33 knots), considerably stronger than typical katabatic regimes and comparable to the Adelie Land winds. As is the case for Adelie Land, a zone of drainage streamline confluence can be seen in Fig. 2. Again, the cold air supply reservoir in the interior of the continent is abnormally large, thereby allowing a persistent and intense katabatic airstream.

This work was funded by the NSF. We thank Ian Allison for furnishing both published¹⁸ and unpublished ANARE sastrugi data.

Received 26 January; accepted 16 April 1987.

1. Egger, J. *J. Atmos. Sci.* **42**, 1859-1867 (1985).
2. James, I. N. in *Second Int. Conf. on Southern Hemisphere Meteorology* 117-118 (American Meteorological Society, Boston, 1986).
3. Parish, T. R. & Bromwich, D. H. *Mon. Weath. Rev.* **114**, 849-860 (1986).
4. Polar Research Board, *The Polar Regions and Climatic Change*, Appendix 8-11 (National Academy Press, Washington DC, 1984).
5. Bromwich, D. H. & Kurtz, D. D. *J. Geophys. Res.* **89**, 3561-3572 (1984).
6. Zwally, H. J., Comiso, J. C. & Gordon, A. L. *Antarctic Res. Ser.* **43**, 203-226 (1985).
7. Gill, A. E. *Deep Sea Res.* **20**, 111-140 (1973).
8. Ball, F. K. in *Antarctic Meteorology: Proc. Symp. Melbourne, Australia, 1959*, 9-16 (Perгамon, Oxford, 1960).
9. Lettau, H. H. & Schwerdtfeger, W. *Antarctic J. U.S.* **2**, 155-158 (1967).
10. Drewry, D. J. *Antarctica: Glaciological and Geophysical Folio* (Scott Polar Research Institute, Cambridge, 1983).
11. Parish, T. R. *Mon. Weath. Rev.* **110**, 84-90 (1982).
12. Schwerdtfeger, W. in *World Survey of Climatology* Vol. 14 (ed. Orvig, S.) 253-355 (Elsevier, Amsterdam, 1970).
13. Mather, K. B. & Miller, G. S. *Notes on Topographic Factors Affecting the Surface Wind in Antarctica, with Special Reference to Katabatic Winds: and Bibliography* (Geophysical Institute, University of Alaska, Fairbanks, 1967).
14. Parish, T. R. *Mon. Weath. Rev.* **112**, 545-554 (1984).
15. Bromwich, D. H. & Kurtz, D. D. *Polar Record* **21**, 137-146 (1982).
16. Bromwich, D. H. *Antarctic J. U.S.* **20**, no. 5, 196-198 (1985).
17. Bromwich, D. H. in *Antarctic Climate Res. No. 1* 13-16 (SCAR-ACR, Antarctic Division, Kingston, Tasmania, 1986).
18. Medhurst, T. G. in *ANARE Res. Notes* 28 (ed. Jacka, T. H.) 174-179 (Antarctic Division, Kingston, Tasmania, 1985).

Structure of the glacial thermocline at Little Bahama Bank

Niall C. Slowey* & William B. Curry†

* WHOI/MIT Joint Program in Oceanography, Woods Hole, Massachusetts 02543, USA

† Department of Geology and Geophysics, Woods Hole Oceanographic Institution, Woods Hole, Massachusetts 02543, USA

Within the thermocline of the western North Atlantic, bathymetric gradients of hydrographic properties are controlled by the lateral movement of water along isopycnal surfaces¹⁻⁴. This movement is driven by air-sea interaction processes: Ekman pumping and surface heat (buoyancy) flux. By affecting the intensity of these processes, glacial-interglacial climatic change should also affect the bathymetric gradients of properties within the thermocline. Benthic foraminifera live on carbonate bank margins that intersect the thermocline. These foraminifera record the hydrographic gradients in their isotopic shell chemistry, providing the means to reconstruct changes in thermocline structure and circulation. We have measured the $\delta^{18}\text{O}$ compositions of a near-surface planktonic foraminifer, *Globigerinoides ruber*, and a shallow-water benthic foraminifer, *Cibicidoides floridanus*, in a core recovered from Little Bahama Bank. *Cibicidoides floridanus* exhibits a glacial-interglacial range in $\delta^{18}\text{O}$ that is 0.5% less than *G. ruber*'s, because individuals of this species lived and calcified ~110 m shallower on the thermocline ~18,000 yr ago. After glacio-eustatic changes in thermocline position are accommodated, we estimate that temperature at 540 m palaeodepth cooled by ~2°C. *Globigerinoides ruber* $\delta^{18}\text{O}$ values suggest that surface water temperature at this